Nitrate sorption by thermally activated Mg/Al chloride hydrotalcite-like compound

Mahamudur Islam [a], Rajkishore Patel [b],*

[a] Department of Chemistry, Purushottam Institute of Engineering and Technology, Rourkela 77 0 034, India
[b] Department of Chemistry, National Institute of Technology, Rourkela 769 008, India

ARTICLE INFO

ABSTRACT

A laboratory study was conducted to investigate the ability of Mg–Al–Cl hydrotalcite-like compound for the removal of nitrate from synthetic nitrate solution. In the present study Mg–Al–Cl hydrotalcite was synthesized by co-precipitation method and was characterized using SEM, XRD, FTIR and TGA–DSC. To know the practical applicability, a detailed removal study of nitrate ion was carried out. The removal of nitrate was 87.6% under neutral condition, using 0.3 g of adsorbent in 100 mL of nitrate solution having initial concentration of 10 mg/L. Adsorption kinetic study revealed that the adsorption process followed first-order kinetics. Adsorption data were fitted to linearly transformed Langmuir isotherm with R^2 (correlation coefficient) > 0.99. Thermodynamic parameters were also calculated to study the effect of temperature on the removal process. In order to understand the adsorption type, equilibrium data were tested with Dubinin–Radushkevich isotherm. The percentage removal was found to decrease gradually with increase in pH and the optimum pH was found to be 6. The process was rapid and equilibrium was established within first 40 min.

1. Introduction

Owing to agricultural and industrial activities, the nitrate concentration in surface and groundwater has increased to such an extent that the admitted standards in drinking water have been largely exceeded in many regions of the world. Several nitrogenous compounds, including ammonia, nitrite and nitrate have been frequently present in drinking water and various types of agricultural, domestic and industrial wastewater [1,2]. US Environmental Protection Agency (EPA) has set the maximum contamination level as 10 mg/L of $NO_3{}^- –N$ [3,4]. Deleterious effects of nitrate on health are well known. Elevated nitrate concentrations in drinking water sources present a potential risk to public health. It can stimulate eutrophication which causes water pollution due to heavy algal growth. Nitrate contaminated water supplies have also been linked to outbreaks of infectious disease [2]. Excess nitrate in drinking water may cause methemoglobinaemia also called a blue baby disease, in newborn infants [5]. Recently it has been found that nitrate ion also causes diabetes [6] and is a precursor of carcinogen.

Background nitrate concentrations in surface waters are usually below 5 ppm, and higher concentrations are often observed in groundwater. Recent surveys revealed that the nitrate levels have

been increased in drinking water supplies in the European Community, the United States, Canada, India, etc. Nitrate is considered to be relatively non-toxic to adults, concentrations greater than 50 ppm can be fatal to infants under 6 months of age. Increased nitrate concentrations in groundwater have caused the shutdown of wells and rendered aquifers unusable as water source. Surface waters also have experienced seasonal nitrate violations. As a result there is renewed interest in the removal of nitrates from raw water. Unfortunately the policy of countermeasures, especially concerning agriculture and environment to limit pollution by nitrates, is efficient only in the long term. So, technical solutions become obligatory. A survey of literature yielded an abundance of information on the technical treatment to remove nitrate from water including ion exchange [7], biological denitrification [8–10], chemical denitrification [11–19], catalytic denitrification [20,21], reverse osmosis [22] and electrodialysis [23]. Current technologies for removal of nitrate like ion exchange, reverse osmosis are not selective to nitrate, generate secondary brine wastes and require frequent media regeneration.

Owing to above difficulties, hydrotalcite-like compounds (HTlcs) were thought to prove a potential adsorbent for the removal of nitrate. Hydrotalcite-like compounds constitute an important class of inorganic materials with desirable properties to remove anionic pollutants from water [24–28]. Hydrotalcites, also known as layered double hydroxides (LDHs) or ionic clays are based upon the brucite $[Mg(OH)_2]$ structure in which some of the divalent cations are replaced by trivalent cations (e.g., Al, Fe, Cr etc.) resulting in

* Corresponding author. Tel.: +91 9437245438/342098; fax: +91 6612462999.
E-mail addresses: smartmintu@gmail.com (M. Islam),
rkpatel@nitrkl.ac.in (R.K. Patel).

a layer charge. This layer charge is counter balanced by anions such as carbonate, nitrate, sulphate or chloride in the interlayer spaces. In hydrotalcites a broad range of compositions are possible of the type $[M_{1-x}^{2+}M_x^{3+}(OH)_2][A^{n-}]_{x/n}\cdot yH_2O$, where M^{2+} and M^{3+} are the di- and trivalent cations in the octahedral positions within the hydroxide layers with x normally between 0.17 and 0.33. A^{n-} is an exchangeable interlayer anion. The degree of anionic exchange in the HTlc depends on the structural characteristics e.g., the nature of the interlayer anion and crystallinity. Exchange conditions like pH and carbonate contamination from environment are also important limitations. Due to the high affinity of HTlcs toward carbonate ion, materials with intercalated carbonate ions have relatively smaller exchange capacities unless being calcined. High pH conditions must be applied to maintain the stability of HTlc, however, OH^- intercalation is competitive in this case.

Although studies have examined the synthesis of various HTlcs and the way in which they interact with various anions, the synthesis of Mg/Al chloride hydrotalcite and its application towards efficient removal of nitrate has not been examined previously. So, the present research was aimed to synthesize, characterize and to study the removal efficiency of nitrate by Mg/Al chloride hydrotalcite. The effect of various parameters on the effectiveness of treating nitrate contaminated water with Mg/Al chloride was unknown. Therefore, in this study, Mg/Al chloride was added to nitrate solutions and the effect of different variables (calcination temperature, dose, time, pH, initial nitrate concentration, effect of other anions etc.) on the removal of nitrate from solution by Mg/Al chloride was examined.

2. Experimental

2.1. Reagents and chemicals

Potassium nitrate, magnesium chloride, aluminum chloride, sodium chloride and sodium hydroxide used in the present study were of analytical grade and were obtained from Merck. 1000 mg/L stock solution of nitrate was prepared by dissolving 1.6305 g of KNO_3 in 1 L distilled water. The required concentration of nitrate solution was obtained by serial dilution of 1000 mg/L nitrate solution. The measuring cylinder, volumetric flask and conical flask and other glassware used were of Borosil.

2.2. Synthesis of Mg–Al–Cl hydrotalcite

Mg–Al–Cl hydrotalcite was prepared by co-precipitation method at pH 10 [29]. In this method two solutions, solution I containing 0.75 M $MgCl_2$ and 0.25 M $AlCl_3$ and solution II containing 1 M NaOH and 1 M NaCl, 200 mL each of these two solutions were added simultaneously to a 1 L beaker containing 100 mL of distilled water at a flow rate of 50 mL/h at 80 °C under vigorous stirring. An inert atmosphere was maintained throughout the addition by purging nitrogen gas from a nitrogen cylinder. The pH of the solution was maintained at 10 by the addition 2 M NaOH. The slurry was then stirred at 90 °C for 24 h. It was then filtered and washed thoroughly with distilled water till the washings were neutral. The precipitate was then dried in nitrogen atmosphere for 8 h. The HTlc obtained was calcined at different temperatures (50–400 °C) in nitrogen atmosphere for 8 h.

2.3. Characterization of Mg–Al–Cl hydrotalcite

BET surface area of the sample was measured using QUANTACHROME Autosorb-I. The sample was degassed at 100 °C in vacuum. Helium was used as carrier gas and the surface area was measured by nitrogen adsorption–desorption method at liquid nitrogen temperature. Thermogravimetric analysis and differential scanning calorimetry (TGA/DSC) analysis was carried out using NETZSCH STA 409C. 30 mg of the sample was used and alumina was used as reference. TGA and DSC curve was obtained from 25 °C to 800 °C at a heating rate of 10 °C/min. Scanning electron micrographs of the sample was obtained by JEOL JSM-6480LV scanning electron microscope. The sample was coated with platinum for 30 s at a current of 50 mA before the SEM micrograph was obtained. Chemical analysis of HTlc was carried out by dissolving 0.5 g of material in 1:1 HCl, followed by the estimation of aluminum by precipitating it with NH_4Cl and NH_4OH. Then the residual solution contained Ca which was estimated by standard EDTA [29,30]. Powder XRD of the material was obtained by using PHILLIPS X'PERT X-ray diffractometer with Cu Kα radiation (35 kV and 30 mA) at a scan rate of 1°/min and was analyzed using standard software provided with the instrument. FTIR of the sample was obtained using PerkinElmer FTIR spectrophotometer (SPECTRUM RX-I).

2.4. Batch experiments

The nitrate adsorption experiments from its aqueous solution by HTlc were carried out using standard 10 mg/L, 50 mg/L and 100 mg/L NO_3^- solution. The adsorption experiments were carried out in 250 mL glass conical flask with stopper by adding 0.1–0.8 g of HTlc in 100 mL of synthetic nitrate solution. Stoppers were provided to avoid change in concentration due to evaporation. All the experiments were carried out at ambient temperature (25 ± 2 °C). After continuous stirring over a magnetic stirrer at about 400 rpm for a predetermined time interval, nitrate concentration was determined by nitrate ion selective electrode (Orion Ionplus Sureflow Nitrate Electrode) and Orion 720 A$^+$ ion analyzer. Two standards were prepared that bracket the expected sample range and which differ in concentration by a factor of 10. Measurements were done by taking 10 mL of each standard and sample into separate 50 mL beaker and 10 mL of nitrate interference suppressor (930710). All the samples and standards were maintained at same temperature to avoid interference due to difference in temperature. A number of parameters such as contact time, adsorbent dose, concentration of nitrate, pH, affecting the adsorption of nitrate ion have been varied widely in order to optimize the removal process.

3. Results and discussion

3.1. Characterization

A number of HTlcs were prepared and were tested for the removal efficiency of nitrate. 0.5 g of each HTlc were added to 100 mL of 100 mg/L nitrate solution and were stirred for 8 h. Then they were filtered and were analyzed for residual nitrate. The results of the study are presented in Table 1. The percentage removal of nitrate was 70.6% for Mg–Al–Cl. It is evident from the table that Mg–Al–Cl exhibited maximum removal of nitrate from synthetic nitrate solution. All other HTlcs used, exhibited a poor nitrate removal efficiency (less than 12%). So, Mg–Al–Cl was selected for further study.

Table 1
Synthesis of various samples of layered double hydroxides (LDHs).

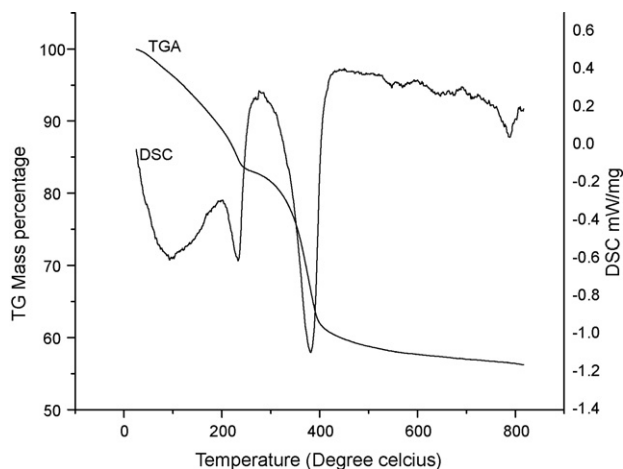| Uncalcined Layered double hydroxides (LDHs)	Percentage removal of nitrate from 100 mg/L solution
Mg–Al–Cl	70.6
Mg–Al–CO₃	3.6
Zn–Cr–Cl	11.2
Mg–Mn–CO₃	3.8
Mg–Cr–Cl	9.8
Ca–Cr–Cl	5.2

Table 2
Effect of calcinations temperature on specific surface area and the removal of nitrate by various samples of layered double hydroxides (LDHs).

| Calcination temperature (in °C)	Specific surface area of different LDHs (m²/g Mg–Al–Cl)	Percentage removal of nitrate from 100 mg/L synthetic nitrate solution by Mg–Al–Cl
50	95.6	70.6
100	106.9	73.3
150	160.2	75.8
200	214.2	78.6
250	225.3	76.6
300	230.6	65.2
350	232.1	55.3
400	235.3	47.4

To study the effect of calcinations temperature on the removal of nitrate, sample of Mg–Al–Cl HTlc was calcined at different temperatures (50–400 °C in nitrogen atmosphere) for 8 h. 0.5 g of calcined samples were added to 100 mL of 100 mg/L nitrate solution and percentage removal of nitrate was studied. The result of the study is presented in Table 2. It is clear from the table that the percentage removal increased with increase in temperature up to 200 °C and then it started to decrease. Maximum percentage removal of 78.6% was obtained with Mg–Al–Cl calcined at 200 °C. So, the above HTlc was calcined at 200 °C and was used for batch studies.

Specific surface area of HTlc calcined at different temperatures was measured using QUANTACHROME Autosorb-I. Result of the study is presented in Table 2. It is evident from the table that the specific surface area (BET) increased with increase in temperature. The BET surface areas of HTlcs calcined at 200 °C were 214.2 m²/g. Though there was further increase in specific surface area with increase in temperature but the percentage removal of nitrate decreased after calcinations at 200 °C (Table 2). This may be due to the structural deformation of HTlcs which takes place, when calcined at higher temperature. Das et al. reported similar effect [29].

TGA and DSC analyses of HTlc were carried out and results are presented in Fig. 1. Three endothermic peaks were found from the DSC analysis of Mg–Al–Cl HTlc. First endothermic process was up to the temperature of 198.15 °C and the corresponding weight loss from TGA analysis was found to be 10.984%. This weight loss was probably due to the physically adsorbed water on the HTlc. Second endothermic process continued up to 249.15 °C and the corresponding weight loss was found to be 5.668%. This may be due to the loss of loosely bound water, strongly bound water and probably due to the
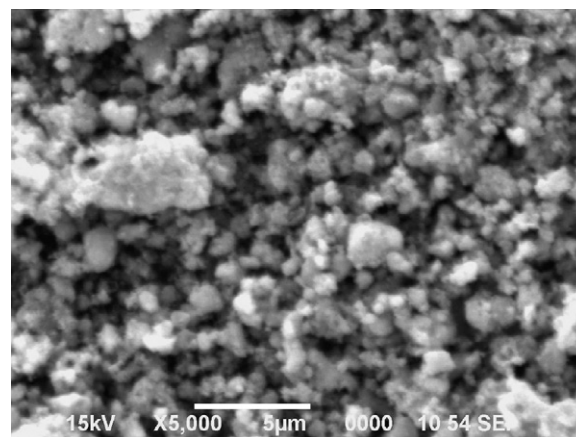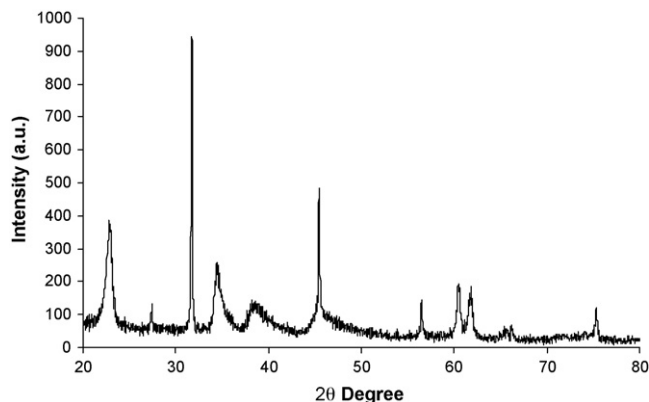

Fig. 2. SEM micrographs of Mg–Al–Cl layered double hydroxide (magnification—5000×, 15 kV).

formation of gaseous HCl. Third endothermic process continued up to 403.15 °C and the corresponding weight loss was 21.290% due to the simultaneous dehydroxylation of lattice OH⁻.

Scanning electron micrograph of Mg–Al–Cl HTlc sample was obtained and is presented in Fig. 2. The structural morphology of the HTlc can be clearly observed from the figure. Chemical analysis of HTlc was carried out in order to calculate the molar ratios of M^{II}:M^{III} present in the HTlc. During the synthesis, M^{II}:M^{III} ratio was taken as 3:1. The Mg:Al ratios were found to be 3.151:1. The M^{II}:M^{III} ratios obtained were almost equal to 3:1. So, chemical analysis of HTlc ascertains the synthesis with required M^{II}:M^{III} ratios. The chemical formula, on the basis of chemical analysis can be suggested as $[Mg_3Al(OH)_8]Cl \cdot xH_2O$.

Powder XRD of calcined HTlc was obtained and the graph is presented in Fig. 3. The difractogram was analyzed with Philips X'Pert High Score software to search for different phases. The results obtained from the analysis indicated that there were not any starting materials present in the HTlc but some of the HTlc formed was converted to oxides of Mg and Al due to calcination. The figure shows sharp and symmetric peaks which gives clear indication that the samples are well crystalline and peak corresponding to (0 0 6), (1 1 0), and (1 1 3) planes are characteristic of clay minerals (HTlc) having layered structure.

FTIR study of Mg–Al–Cl HTlc and HTlc recovered after adsorption were carried out in order to know the presence of different groups, structures and adsorption of nitrate onto HTlc. FTIR spectrum of Mg–Al–Cl is presented in Fig. 4. An intense broad band at 3473 cm⁻¹ may be due to superimposition of deformational vibrations of physically adsorbed water [31], vibrations of structural OH⁻ groups [32]

Fig. 1. Thermogravimetric analysis and differential scanning calorimetry of Mg–Al–Cl layered double hydroxide.

Fig. 3. XRD pattern of Mg–Al–Cl layered double hydroxide.
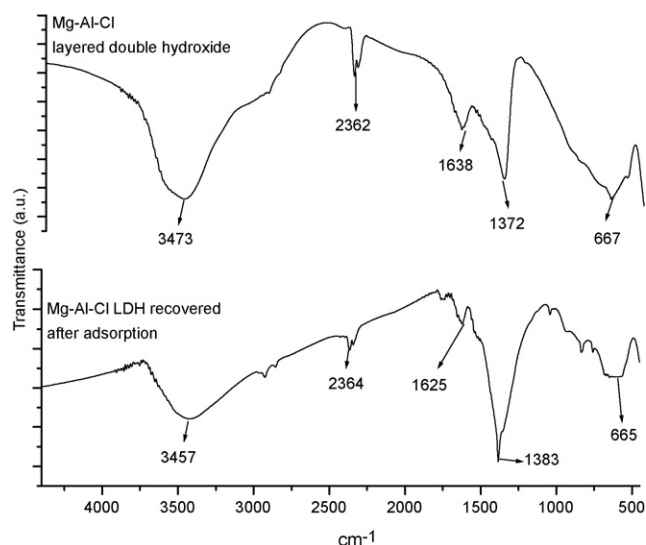
Fig. 4. FTIR pattern of Mg–Al–Cl LDH and Mg–Al–Cl LDH recovered after adsorption.

Fig. 6. Time versus percentage removal of lead, Mg–Al–Cl LDH, with initial concentration of 10 mg/L, 50 mg/L and 100 mg/L.

and characteristic valent vibration of HO···OH in hydrotalcite [33]. The peak at 2362 cm^{-1} is apparently due to CO$_2$ background of the measurement system [34]. The peak at 1638 cm^{-1} (bending vibration of δ HOH) may be assigned to the adsorbed interlayer water. The band at 1372 cm^{-1} is most probably due to carbonate anion which might have formed due to absorption of atmospheric CO$_2$ gas. A characteristic vibration of hydrotalcite is indicated by a peak at 667 cm^{-1} [33]. FTIR spectrum of Mg–Al–Cl recovered after adsorption is presented in Fig. 4. A peak at 3457 cm^{-1} was observed, which may be due to physically adsorbed water [31], vibrations of structural OH$^-$ groups [32]. A peak at 2364 cm^{-1} is due to CO$_2$ background of the measurement system. Band at 1625 cm^{-1} (bending vibration of δ HOH) may be due to the adsorbed interlayer water. A peak at 1383 cm^{-1} is associated with the antisymmetric stretching mode of nitrate (v_3) [35,36] which ascertains the adsorption of nitrate onto Mg–Al–Cl HTlc. A broad band at 665 cm^{-1} is most probably due to superposition of the characteristic bonds of HTlc.

3.2. Removal study of nitrate by batch mode experiments

3.2.1. Effect of adsorbent dose and pH

The effect of variation of adsorbent dose on percentage removal of nitrate from aqueous solution with HTlc used in this study is graphically shown in Fig. 5. It is evident from the figure that the removal of nitrate increased from 67.2% to 87.6%, 64.4% to
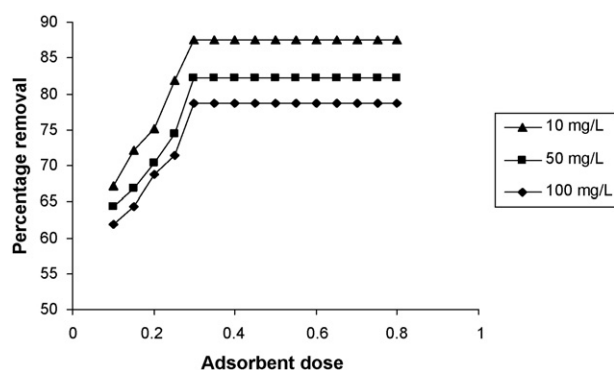

Fig. 5. Adsorbent dose versus percentage removal of nitrate by Mg–Al–Cl LDH with initial concentration of 10 mg/L, 50 mg/L and 100 mg/L.
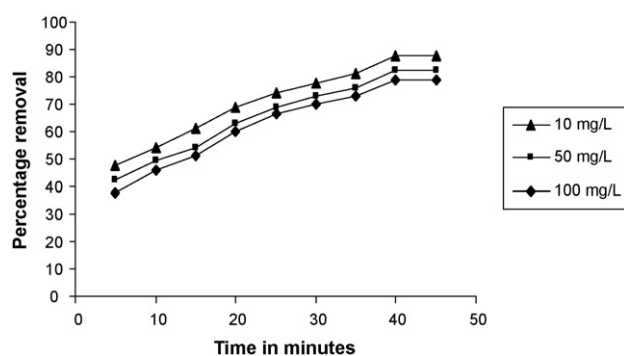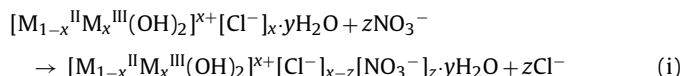
82.2% and 61.9% to 78.6% for 0.1–0.8 g of HTlc in 100 mL of synthetic nitrate solution of initial concentration, 10 mg/L, 50 mg/L and 100 mg/L respectively. However it is observed that after dosage of 0.3 g/100 mL, there was no significant change in percentage removal of nitrate. This may be due to the overlapping of active sites at higher dosage. So, there was not any appreciable increase in the effective surface area resulting due to the conglomeration of exchanger particles [37]. So, 0.3 g/100 mL was considered as optimum dose and was used for further study.

The removal of nitrate at different pHs was studied and was found that the percentage removal of nitrate by Mg–Al–Cl HTlc decreased from 87.6% to 77.9%, 82.2% to 74.2% and 78.6% to 69.9% for increase in pH from 6 to 12, for initial nitrate concentration of 10 mg/L, 50 mg/L and 100 mg/L respectively. It is evident from the above data that there was slight decrease (8–10%) in percentage removal with increase in pH of the solution. This may be due to the fact that with increase in pH, OH$^-$ concentration in the solution increases, which competes with nitrate ion. The above data suggests that the optimum pH for removal of nitrate was 6. Anion exchange involves the breaking up of the electrostatic interactions as well as the hydrogen bonds between the hydroxide layers and the outgoing anion and the reformation of these bonds with the incoming anions. The most probable general mechanism for anion exchange reaction in HTlc can be suggested as below:

$$[M_{1-x}{}^{II}M_x{}^{III}(OH)_2]^{x+}[Cl^-]_x \cdot yH_2O + zNO_3{}^-$$
$$\rightarrow [M_{1-x}{}^{II}M_x{}^{III}(OH)_2]^{x+}[Cl^-]_{x-z}[NO_3{}^-]_z \cdot yH_2O + zCl^- \qquad (i)$$

3.2.2. Effect of contact time and adsorption kinetics

Adsorption of nitrate at different contact times was studied for initial nitrate concentration of 10 mg/L, 50 mg/L and 100 mg/L keeping all other parameters constant. The result is presented in Fig. 6. The percentage removal was found to increase from 47.6% to 87.6%, 42.6% to 82.2% and 37.8% to 78.6% for a contact time of 5–40 min and initial nitrate concentration of 10 mg/L, 50 mg/L and 100 mg/L respectively. It is clear from the figure that about 40% removal took place within first 5 min and equilibrium was established after 40 min. The change in the rate of removal might be due to the fact that initially replaceable chloride ion was present in all adsorbent sites and the solute concentration gradient was high. Later, the nitrate uptake rate by adsorbent was decreased significantly, due to the decrease in number of replaceable chloride ions in adsorption sites as well as decrease in nitrate concentration. Decreased removal rate, particularly, towards the end of experiments, indicates the possible monolayer formation of nitrate ion on the outer surface.

Adsorption of nitrate ion was rapid for the first 5 min and its rate slowed down as the equilibrium approached. The rate constant K_{ad} for sorption of nitrate was studied by Lagergren rate equa-

Table 3
Rate constants (K_{ad}) obtained from the graph for HTlc with different initial concentrations of nitrate.

Initial concentration	Slope	Intercept	Rate constant, K_{ad} (min^{-1})	R^2
10 mg/L	−0.02683	0.30714	0.06180	0.987
50 mg/L	−0.02717	1.01511	0.06258	0.980
100 mg/L	−0.02861	1.33021	0.06589	0.984
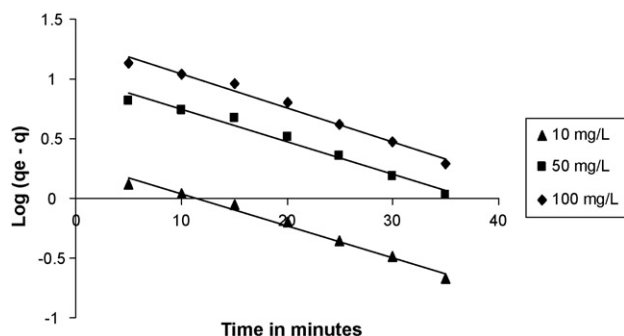
Fig. 7. Linear plot of Lagergren rate equation using Mg–Al–Cl LDH, time versus log ($q_e - q$) with initial lead concentration of 10 mg/L, 50 mg/L and 100 mg/L.

Fig. 8. Linear plot of Weber–Morris equation using Mg–Al–Cl LDH, square root of time versus q_e with initial nitrate concentration of 10 mg/L, 50 mg/L and 100 mg/L.

tion [38,39] for initial lead concentration of 10 mg/L, 50 mg/L and 100 mg/L:

$$\log(q_e - q) = \log q_e - K_{ad}\left(\frac{t}{2.303}\right) \qquad (ii)$$

where q_e and q (both in mg/g) are the amounts of nitrate adsorbed at equilibrium and at time 't', respectively. The plots of log ($q_e - q$) versus 't' at different time intervals was almost linear, indicates the validity of Lagergren rate equation of first-order kinetics (Fig. 7). The adsorption rate constant (K_{ad}), calculated from the slope of the above plot is presented in Table 3.

3.2.3. Intraparticle diffusion rate constant

In order to test the existence of intraparticle diffusion in the adsorption process, the amount of nitrate sorbed per unit mass of adsorbents, q at any time t, was plotted as a function of square root of time ($t^{1/2}$). The rate constant for intraparticle diffusion was obtained using Weber–Morris equation given as follows [40]:
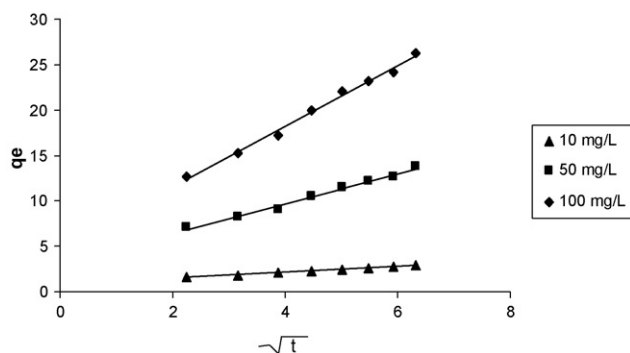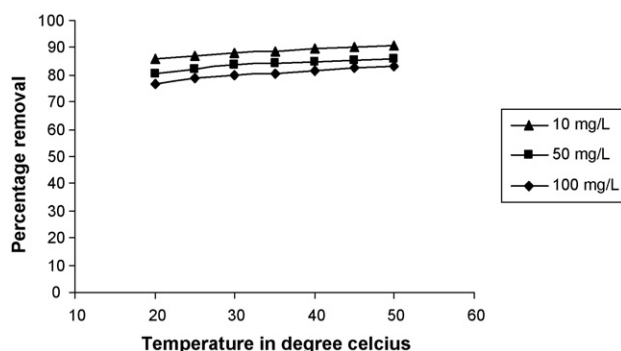
$$q = K_p t^{1/2} + C \qquad (iii)$$

where q is the amount of nitrate adsorbed in milligram per gram of adsorbent, K_p is the intraparticle diffusion rate constant and 't' is the agitation time in minutes. Due to stirring there is a possibility of transport of nitrate species from the bulk into pores of the HTlc as well as adsorption at outer surface of the HTlc. The rate-limiting step may be either adsorption or intraparticle diffusion.

The results obtained are presented in Table 4 and graphically shown in Fig. 8. The rate constants (K_p) for intraparticle diffusion for various initial concentrations of nitrate solution were determined from the slope of respective plots. It is evident from the graph that, the plots were straight lines but the *y*-intercept of the plots were nonzero (not passing through the origin) thus indicating that intraparticle diffusion is not the sole rate-limiting factor

for the adsorption of nitrate onto HTlc. Particles always diffuse from areas of high concentration to areas of low concentration. The difference between the concentrations of a substance in one area compared to another area is the concentration gradient. The direction of the passage of particles through the channel is also dependent on concentration gradients. In the present study, the intraparticle diffusion may be regarded as concentration diffusion because the values of K_p in Table 4 show increase in K_p with the increase in nitrate concentration (concentration gradient) [41].

3.2.4. Effect of temperature

The effect of temperature on the adsorption of nitrate with initial concentration 10 mg/L, 50 mg/L and 100 mg/L onto Mg–Al–Cl HTlc was studied using optimum adsorbent dose and the results are presented as percentage removal of nitrate versus temperature (Fig. 9). The percentage removal of nitrate with initial concentration 10 mg/L, increased from 85.6% to 90.5%, the percentage removal of nitrate with initial concentration 50 mg/L, increased from 80.2% to 85.7% and the percentage removal of nitrate with initial concentration 100 mg/L, increased from 76.8% to 83.3% for 20–50 °C temperature. It is evident from the figure that, at the temperature of 20 °C the removal was more than 75% (initial nitrate concentration of 10 mg/L, 50 mg/L and 100 mg/L) and with increase in temperature, the percentage removal increased slowly and reached almost 90% (initial nitrate concentration of 10 mg/L), which indicates the endothermic nature of the process.

Table 4
Intraparticle diffusion rate constants obtained from Weber–Morris equation for different initial concentrations of nitrate.

Initial concentration	Slope	Intercept	Rate of pore diffusion (K_p)	R^2
10 mg/L	0.31733	0.85085	0.31733	0.992
50 mg/L	1.59388	3.30510	1.59388	0.988
100 mg/L	3.24081	5.21803	3.24081	0.990

Fig. 9. Temperature versus percentage removal of nitrate with Mg–Al–Cl LDH, initial nitrate concentration of 10 mg/L, 50 mg/L and 100 mg/L.

Table 5
Thermodynamic parameters using Mg–Al–Cl LDH, synthetic nitrate solution of 10 mg/L, 50 mg/L and 100 mg/L.

Initial nitrate concentration (mg/L)	ΔH (kJ mol^{-1})	ΔS (kJ K mol^{-1})	ΔG (kJ mol^{-1})							R^2
			20 °C	25 °C	30 °C	35 °C	40 °C	45 °C	50 °C	
10	12.912	0.069	−0.987	−1.560	−2.133	−2.706	−3.280	−3.853	−4.426	0.982
50	10.549	0.058	−1.231	−1.797	−2.364	−2.930	−3.496	−4.062	−4.628	0.961
100	10.361	0.055	−1.789	−2.294	−2.798	−3.303	−3.808	−4.313	−4817	0.989

This was further supported by calculating thermodynamic parameters. The change in free energy (ΔG), enthalpy (ΔH) and entropy (ΔS) of adsorption were calculated using the following equations [38,39]:

$$\log K_C = \frac{\Delta S}{2.303R} - \frac{\Delta H}{2.303RT} \tag{iv}$$

$$\Delta G = \Delta H - T\Delta S \tag{v}$$

where ΔS and ΔH are the changes in entropy and enthalpy of adsorption, respectively. A plot of $\log K_C$ versus $1/T$ for initial nitrate concentration of 10 mg/L, 50 mg/L and 100 mg/L was linear and is represented graphically in Fig. 10.
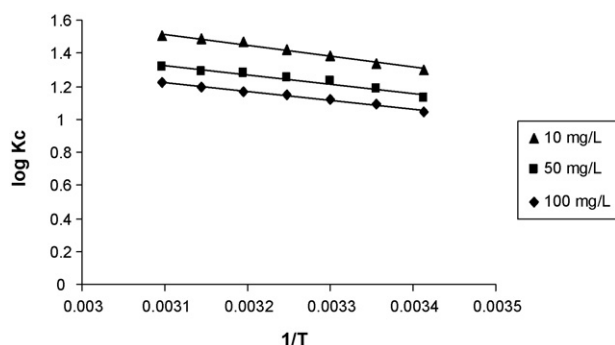
The K_C value was calculated using the following equation [39]:

$$K_C = \frac{C_1}{C_2} \tag{vi}$$

where C_1 is the amount of nitrate ion adsorbed per unit mass of HTlc and C_2 is the concentration of nitrate in aqueous phase. Values of ΔH and ΔS were evaluated from the slope and intercept of Van't Hoff plots and represented in Table 5. The positive values of ΔS indicate some structural changes in the adsorbent and also reflect the affinity of the adsorbent for nitrate species. The positive value of entropy (ΔS) indicates the increase in randomness of the ongoing. During the adsorption of nitrate, the chloride ions (which are displaced by the nitrate ions) gain more entropy than is lost by adsorbate species, thus increasing the randomness in the system. Negative value of ΔG at each temperature indicates the spontaneity of ongoing adsorption. A decrease in values of ΔG with the increase in temperature suggests more spontaneity of nitrate adsorption at higher temperature. The endothermic nature of the process was once again confirmed by the positive value of enthalpy (ΔH). Positive value of enthalpy (ΔH) suggests that entropy is responsible for making the ΔG value negative. So, the adsorption process was spontaneous, since the entropy contribution was much larger than that of enthalpy.

3.2.5. Effect of initial concentration and adsorption isotherms

To investigate the effect of initial nitrate concentration on nitrate adsorption onto Mg–Al–Cl HTlc, batch mode experiments were performed at ambient temperature (25 ± 2 °C). The initial concentration of nitrate solution was varied from 10 mg/L to 100 mg/L

with optimum adsorbent dose. It is evident from the result that the percentage removal of nitrate decreased from 87.6% to 78.6% for initial nitrate concentration of 10–100 mg/L. The results indicate that there is a reduction in nitrate adsorption, owing to the lack of available active sites required for the high initial concentration of nitrate. The higher uptake of nitrate at low concentration may be attributed to the availability of more active sites on the surface of the adsorbent for lesser number of adsorbate species.

The adsorption data were fitted to linearly transformed Langmuir isotherm. The linearized Langmuir equation, which is valid for monolayer sorption onto a surface with finite number of identical sites, is given by the following equation [38,39]:

$$\frac{1}{q_e} = \frac{1}{q_0 bC_e} + \frac{1}{q_0} \tag{vii}$$

where q_0 is the maximum amount of the nitrate ion per unit weight of Mg–Al–Cl HTlc to form a complete monolayer on the surface (adsorption capacity) C_e denotes equilibrium adsorbate concentration in solution, q_e is the amount adsorbed per unit mass of adsorbent, and b is the binding energy constant. The linear plot of $1/C_e$ versus $1/q_e$ (Fig. 11) with $R^2 = 0.998$ indicates the applicability of Langmuir adsorption isotherm. The values of Langmuir parameters, q_0 and b are 41.77827 mg/g and 0.06040 L/mg, respectively.

In order to predict the adsorption efficiency of the adsorption process, the dimensionless equilibrium parameter was determined by using the following equation [38,39]:

$$r = \frac{1}{1 + bC_0} \tag{viii}$$

where C_0 is the initial nitrate concentration. Values of $r < 1$ represent favorable adsorption. The r-value for initial concentration of 10 mg/L, 50 mg/L and 100 mg/L was found to be 0.62344, 0.24875 and 0.14204 respectively. The values indicated a favorable system.

It is known that the Langmuir and Freundlich adsorption isotherm constant do not give any idea about the adsorption mechanism. In order to understand the adsorption type, equilibrium data were tested with Dubinin–Radushkevich isotherm [38]. The linearized D.R. equation can be written as:

$$\ln q_e = \ln q_m - K\varepsilon^2 \tag{ix}$$

where ε is the Polanyi potential, and is equal to $RT \ln(1 + 1/C_e)$, q_e is the amount of nitrate adsorbed per unit mass of adsorbent, q_m is

Fig. 10. Van't Hoff plots, $\log K_C$ versus $1/T$ for Mg–Al–Cl LDH, initial nitrate concentration of 10 mg/L, 50 mg/L and 100 mg/L.
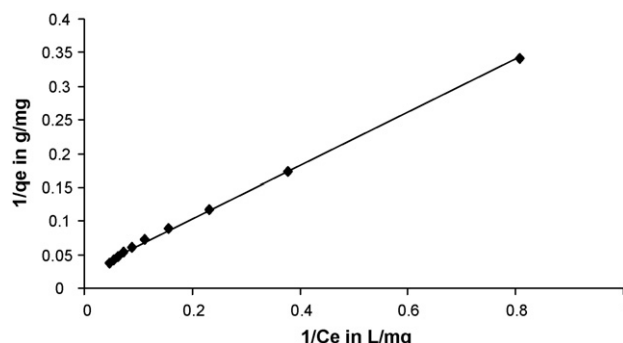
Fig. 11. Langmuir adsorption isotherm, $1/C_e$ versus $1/q_e$ for Mg–Al–Cl LDH.

the theoretical adsorption capacity, C_e is the equilibrium concentration of nitrate, K is the constant related to adsorption energy, R is universal gas constant and T is the temperature in Kelvin.

Fig. 12 shows the plot of $\ln q_e$ against ε^2, which was almost linear with correlation coefficient, $R^2 = 0.914$. D.R. isotherm constants K and q_m were calculated from the slope and intercept of the plot, respectively. The value of K was found to be 0.00256 mol^2 kJ^{-2} and that of q_m was 0.01912 g/g. The mean free energy of adsorption (E) was calculated from the constant K using the relation [39]:

$$E = (2K)^{-1/2} \tag{x}$$

It is defined as the free energy change when 1 mol of ion is transferred to the surface of the solid from infinity in solution. The value of E was found to be 13.95364 kJ mol^{-1}. The value of E is very useful in predicting the type of adsorption and if the value is less than 8 kJ mol^{-1}, then the adsorption is physical in nature and if it is in between 8 kJ mol^{-1} and 16 kJ mol^{-1}, then the adsorption is due to exchange of ions [39]. The value found in the present study was in between 8 kJ mol^{-1} and 16 kJ mol^{-1}. So, the adsorption can be best explained as exchange of ions.

3.2.6. Effect of competitive ions

The adsorption results discussed above were obtained taking nitrate ion only. However, in reality the nitrate contaminated water contains several other anions which can equally compete in the adsorption process. In order to see effect of interfering ions on adsorption of nitrate, a mixture of known quantities of commonly occurring anions in water, viz., phosphate, chloride, carbonate and sulphate were added to nitrate solutions. The initial concentration of nitrate was fixed at 10 mg/L, 50 mg/L and 100 mg/L while the initial concentration of other anions varied from 10 mg/L to 100 mg/L. The dependence of such ions on adsorption of nitrate at varying concentrations of competitive anions was studied and was found that these anions reduced the adsorption of nitrate appreciably. The anions reduced the nitrate adsorption in the order of, carbonate > phosphate > chloride > sulphate. From above, it is evident that carbonate has maximum and sulphate has least effect on the removal of nitrate by HTlc. It was observed that there was about 25% reduction in the percentage removal of nitrate by carbonate. This may be due to the strong tendency of HTlc to form corresponding carbonate.

3.2.7. Desorption and regeneration studies

Desorption and regeneration studies give an idea about the nature of adsorption. Chemisorption exhibits poor desorption, it may be due to fact that in chemisorption the adsorbate species are held firmly to the adsorbent with comparatively stronger bonds. Regeneration studies were carried out in order to know the
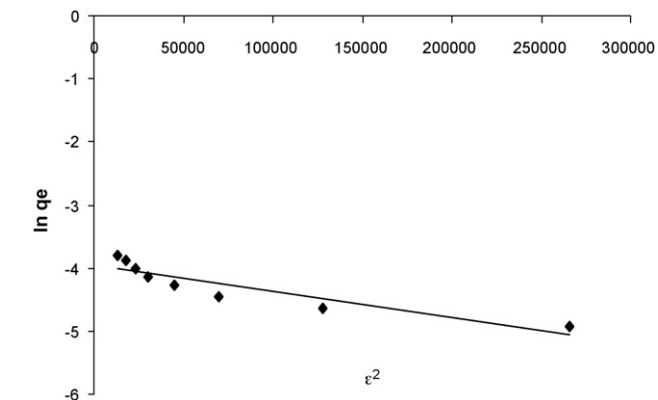
reusability of the HTlc. The results of the studies indicated that the desorption of the adsorbed nitrate in neutral distilled water resulted about 1.01%, 1.02% and 1.03% for initial concentration of 10 mg/L, 50 mg/L and 100 mg/L respectively. It is evident from the low desorption values, that the adsorption of nitrate onto HTlc was chemical in nature, which is in well agreement with the previous data.

At the end of the adsorption process, when the working capacity of an adsorbent is exhausted, it has to be regenerated. Adsorbents are usually regenerated with acid or alkali solution. In the present study, adsorbent (HTlc) was unstable in acidic medium. So, the regeneration study was carried out at pH of 8, 10 and 12 and it was observed that regeneration was less than 2% at different pHs. Regeneration studies were also carried out using 1 M, 2 M and 4 M NaCl and it was observed that regeneration was less than 1%. So, once HTlc-nitrate is formed it is difficult to regenerate.

4. Conclusion

Mg–Al–Cl hydrotalcite was synthesized by magnesium chloride, aluminum chloride, sodium chloride and sodium hydroxide by co-precipitation method. Synthesis was ascertained by adopting various characterizing methods like SEM, XRD, FTIR, TGA–DSC and chemical analysis. Mg–Al–Cl hydrotalcite exhibited much greater specific surface area and which increased with increase in calcination temperature. The adsorption of nitrate from aqueous solution by Mg–Al–Cl hydrotalcite was found to occur readily. Adsorption of nitrate was found to follow first-order kinetics. The effect of other anions were also studied and was found that the anions reduced the nitrate adsorption in the order of carbonate > phosphate > chloride > sulphate. The percentage removal was found to decrease with increase in pH and the optimum pH was found to be 6. A regeneration study of the material was also carried out and was found that the Mg–Al–Cl hydrotalcite cannot be easily regenerated and reused. The percentage regeneration was less than 2%. The removal of nitrate with Mg–Al–Cl hydrotalcite was very efficient and can bring down the nitrate concentration to its permissible limit. The process can be employed as a primary step for the removal of nitrate to meet permissible limit of nitrate in surface and groundwater.

Fig. 12. D–R adsorption isotherm, $\ln q_e$ versus ε^2 for Mg–Al–Cl LDH.

References

[1] H.S. Peavy, D.R. Rowe, G. Tchobanoglous, Environmental Engineering, McGraw-Hill Book Company, New York, 1985, p. 696.
[2] S.H. Lin, C.L. Wu, Removal of nitrogenous compounds from aqueous solution by ozonation and ion exchange, Water Res. 30 (8) (1996) 1851–1857.
[3] M.N. Almasri, J.J. Kaluarachchi, Assessment and management of longterm nitrate pollution of ground water in agriculture-dominated watersheds, J. Hydrol. 295 (2004) 225–245.
[4] A.H. Wolfe, J.A. Patz, Reactive nitrogen and human health: acute and long-term implications, Ambio 31 (2002) 120–125.
[5] Z. Feleke, Y. Sakakıbara, A bio-electrochemical reactor coupled with adsorber for the removal of nitrate and inhibitory pesticide, Water Res. 36 (12) (2002) 3092–3102.
[6] T.N. Kostraba, E.C. Gay, M. Rewers, R.F. Hamman, Nitrate levels in community drinking waters and risk of IDDM. An ecological analysis, Diab. Care 15 (1992) 1505–1508.
[7] A. Pintar, J. Batista, Improvement of an integrated ion-exchange/catalytic process for nitrate removal by introducing a two-stage denitrification step, Appl. Catal. B: Environ. 63 (2006) 150–159.

[8] B. Moreno, M.A. Gomez, A. Ramos, J. Gonzalez-Lopez, E. Hontoria, Influence of inocula over start up of a denitrifying submerged filter applied to nitrate contaminated groundwater treatment, J. Hazard. Mater. B127 (2005) 180–186.

[9] M.A. Gomez, J. Gonzalez-Lopez, E. Hontoria-Garcıa, Influence of carbon source on nitrate removal of contaminated groundwater in a denitrifying submerged filter, J. Hazard. Mater. 80 (1–3) (2000) 69–80.

[10] B. Moreno, M.A. Gomez, J. Gonzalez-Lopez, E. Hontoria, Inoculation of a submerged filter for biological denitrification of nitrate polluted groundwater: a comparative study, J. Hazard. Mater. 117 (2–3) (2005) 141–147.

[11] M. Kumar, S. Chakraborty, Chemical denitrification of water by zero-valent magnesium powder, J. Hazard. Mater. B 135 (2006) 112–121.

[12] A.P. Murphy, Chemical removal of nitrate from groundwater, Nature 350 (1991) 223–225.

[13] Y.H. Huang, T.C. Zhang, Effects of low pH on nitrate reduction by iron powder, Water Res. 38 (2004) 2631–2642.

[14] Y.H. Huang, T.C. Zhang, Kinetics of nitrate reduction by iron at near neutral pH, J. Environ. Eng. 128 (2002) 604–610.

[15] Y. Chen, C. Li, S. Chen, Fluidized zero valent iron bed reactor for nitrate removal, Chemosphere 59 (2005) 753–759.

[16] J. Kielemoes, P. de Boever, W. Verstraete, Influence of denitrification on the corrosion of iron and stainless steel powder, Environ. Sci. Technol. 34 (2000) 663–671.

[17] J.C. Fanning, The chemical reduction of nitrate in aqueous solution, Coord. Chem. Rev. 199 (2000) 159–179.

[18] A. Agrawal, P.G. Tratnyek, Reduction of nitro aromatic compounds by zero-valent iron metal, Environ. Sci. Technol. 30 (1996) 153–160.

[19] F. Cheng, R. Muftikian, Q. Fernando, N. Korte, Reduction of nitrate to ammonia by zero valent iron, Chemosphere 35 (1997) 2689–2695.

[20] A. Pintar, J. Batista, J. Levec, Integrated ion exchange/catalytic process for efficient removal of nitrates from drinking water, Chem. Eng. Sci. 56 (2001) 1551–1559.

[21] A. Pintar, J. Batista, Catalytic hydrogenation of aqueous nitrate solutions in fixed-bed reactors, Catal. Today 53 (1999) 35–50.

[22] J.J. Schoeman, A. Steyn, Nitrate removal with reverse osmosis in a rural area in South Africa, Desalination 15 (5) (2003) 15–26.

[23] A. Elmidaoui, M.A. Menkouchi Sahli, M. Tahaikt, L. Chay, M. Taky, M. Elmghari, M. Hafsi, Selective nitrate removal by coupling electrodialysis and a bioreactor, Desalination 153 (2002) 389–397.

[24] A. Nedim, B. Zumreoglu-Karan, A. Temel, Boron removal by hydrotalcite-like, carbonate-free Mg–Al–NO$_3$$^-$ LDH and a rationale on the mechanism, Micropor. Mesopor. Mater. 98 (2007) 1–5.

[25] S.P. Paredes, G. Fetter, P. Bosch, S. Bulbulian, Iodine sorption by microwave irradiated hydrotalcites, J. Nucl. Mater. 359 (2006) 155–161.

[26] R.L. Frost, A.W. Musumeci, Nitrate absorption through hydrotalcite reformation, J. Colloid Interface Sci. 302 (2006) 203–206.

[27] T. Kameda, YoshiokaF T., T. Hoshi, M. Uchida, A. Okuwaki, The removal of chloride from solutions with various cations using magnesium–aluminum oxide, Sep. Purif. Technol. 42 (2005) 25–29.

[28] A.E. Palomares, J.G. Prato, F. Rey, A. Corma, Using the "memory effect" of hydrotalcites for improving the catalytic reduction of nitrates in water, J. Catal. 221 (2004) 62–66.

[29] D.P. Das, J. Das, K. Parida, Physicochemical characterization and adsorption behavior of calcined Zn/Al hydrotalcite-like compound (HTlc) towards removal of fluoride from aqueous solution, J. Colloid Interface Sci. 261 (2003) 213–220.

[30] A.I. Vogel, A Text Book of Quantitative Inorganic Analysis, Longman, London, 1969, pp. 433–434.

[31] G. Allegra, G. Ronca, Crystal powder statistics. II. Line profiles in diffraction spectra of identical crystals and of Gaussian samples, Crystal size distributions Acta Cryst. A 34 (1978) 1006–1013.

[32] D. Roy, R. Roy, E. Osborn, The system MgO–Al$_2$O$_3$–H$_2$O and influence of carbonate and nitrate ions on the phase equilibria, Am. J. Sci. 251 (1953) 337–361.

[33] R. Allmann, Double layer structures with brucite-like ions [Me(II)$_{(1-x)}$Me(III)$_x$(OH)$_2$]$^{x+}$, Chimia 24 (3) (1970) 99–108.

[34] R.S. Zhai, A. Das, C.-K. Hsu, C.-C. Han, T. Canteenwala, L.Y. Chiang, T.J. Chuang, Polymeric fullerene oxide films produced by decomposition of hexanitro[60]fullerene, Carbon 42 (2004) 395–403.

[35] B.J. Hathway, A.E. Underhill, The infrared spectra of some transition-metal perchlorates, J. Chem. Soc. (1961) 3091–3096.

[36] J.T. Kloprogge, L. Hickey, R.L. Frost, The effect of varying synthesis conditions on zinc chromium hydrotalcite: a spectroscopic study, Mater. Chem. Phys. 89 (1) (2005) 99–109.

[37] H. Tahir, Comparative trace metal contents in sediments and the removal of chromium using Zeolite-5A, EJEAF Chem. 4 (4) (2005) 1021–1032.

[38] M. Islam, R.K. Patel, Evaluation of removal efficiency of fluoride from aqueous solution using quick lime, J. Hazard. Mater. 143 (2007) 303–310.

[39] M. Islam, R.K. Patel, Polyacrylamide thorium (IV) phosphate as an important lead selective fibrous ion exchanger: synthesis, characterization and removal study, J. Hazard. Mater. 156 (2008) 509–520.

[40] A.K. Yadav, C.P. Kaushik, A.K. Haritash, A. Kansal, N. Rani, Defluoridation of groundwater using brick powder as an adsorbent, J. Hazard. Mater. 128 (2–3) (2006) 289–293.

[41] K. Kadirvelu, C. Faur-Brasquet, P. Le Cloiree, Removal of Cu(II) Pb(II) and Ni(II) by adsorption onto activated carbon cloths, Langmuir 16 (2000) 8404–8409.